Defect structure of MBE-grown GaCrN diluted magnetic semiconductor films



2011 J. Phys.: Conf. Ser. 262 012066

(http://iopscience.iop.org/1742-6596/262/1/012066)

Journal of Physics: Conference Series **262** (2011) 012066 doi:10.1088/1742-6596/262/1/012066

# Defect structure of MBE-grown GaCrN diluted magnetic semiconductor films

**A Yabuuchi[1], M Maekawa[1], A Kawasuso[1], S Hasegawa[2], Y K Zhou[2] and H Asahi[2]**
[1]ASRC, Japan Atomic Energy Agency, 1233, Watanuki, Takasaki, Gunma 370-1292, Japan
[2] ISIR, Osaka University, 8-1, Mihogaoka, Ibaraki, Osaka 567-0047, Japan

E-mail: yabuuchi.atsushi@jaea.go.jp

**Abstract.** Effects of growth temperature and Si doping on the formation of vacancy defects in molecular beam epitaxy GaCrN films have been studied by positron annihilation spectroscopy. No vacancy defects were detected in the GaCrN films grown at 700°C. In the undoped GaCrN film grown at 540°C, vacancy clusters with sizes of $V_8$ to $V_{12}$ were responsible for positron trapping. Vacancy clusters were much reduced by Si doping, but complexes related to nitrogen vacancies still survived.

## 1. Introduction

Chromium-doped GaN is one of the expected GaN-based diluted magnetic semiconductor (DMS) working at room-temperature [1-3]. To obtain the ferromagnetic property, it is important to substitute Ga atoms with high concentration of Cr atoms. However, heavy Cr doping results in the precipitation of CrN secondary phase at normal growth temperature. To avoid the formation of CrN secondary phase, low temperature molecular beam epitaxy (MBE) growth may be a promising manner. In this case, the introduction of vacancy-type defects during MBE growth is anticipated. Recent first-principle calculation studies proposed that the vacancy-type defects in the DMS materials might play an important role for ferromagnetism [4]. Therefore, it is important to investigate the vacancy-type defect structure of the DMS materials. Positron annihilation spectroscopy (PAS) is a capable tool to detect vacancy-type defects. Many PAS studies have been performed on GaN as opto-materials [5]. However, only a few PAS studies are reported about the defect structure of the GaN-based DMS materials [6]. In this study, the defect structure of low-temperature MBE-grown GaCrN films has been probed by a slow positron beam.

## 2. Experiment

Samples used in this study were GaN-cap(4 nm)/GaCrN(500 nm)/GaN-buffer(40 nm) structures grown by radio frequency (RF) plasma assisted MBE method on commercial GaN templates (2 μm) grown by metal-oxide chemical vapour deposition (MOCVD) methods. The GaN-cap layers and GaN-buffer layers were prepared at 700 °C. The GaCrN (with Cr concentration of 0.7 %) layers were grown at 700 °C or 540 °C with the growth rate of 200 nm/h. The Ga flux, $N_2$ flow rate and RF plasma power were kept constant at $1.6\times10^{-7}$ Torr, 1.5 sccm and 180 W, respectively. These are referred as HT-GaCrN or LT-GaCrN. In both growth temperatures, Si-doped GaCrN films ([Si]=$10^{18}$ $cm^{-3}$) were also prepared. The LT- GaCrN samples were eventually heated at 700 °C where the cap layers were grown.

Monoenergetic positron beam with energy (E) of 0.2-30 keV were implanted into the above samples and the Doppler broadening of annihilation radiation (DBAR) measurements were carried out. The DBAR spectra were characterized by S parameter with an energy window of 511±0.8 keV. All the S parameters were normalized to that obtained for the GaN template. To examine the electron-positron momentum distribution in detail, the coincidence DBAR measurements were also performed. Positron annihilation lifetime measurements were also done with a pulsed positron beam.

## 3. Calculation of positron annihilation characteristics

To interpret experimental positron lifetime and DBAR data, theoretical calculations were carried out. Positron lifetimes of perfect GaN and some vacancy defects were calculated based on the atomic superposition method developed by Puska et al. [7] with the Borónski–Niemnen enhancement factor [8]. The supercell includes 64 Ga atoms and 64 N atoms, i.e., it is a 4×2×2 wurtzite conventional unit cell. The lattice constants were a=3.18Å and c=5.17Å.

The DBAR spectra were calculated within the local density approximation [7]. The valence electron wavefunctions were calculated with the projector augmented-wave (PAW) method [9] using the ABINIT4.6.4 code [10]. The potentials and projectors were generated using the ATOMPAW code [11]. The valence electron configurations were $3d^{10}4s^24p^1$, $2s^22p^3$, $3s^23p^63d^54s^1$, $3s^23p^2$ for Ga, N, Cr and Si atoms, respectively. A supercell including 32 Ga and 32 N atoms with a 2×2×2 conventional wurtzite unit cell was constructed as a GaN crystal. For the calculation of vacancy defects, the lattice relaxations were introduced by the molecular dynamics simulation installed in the code. The cut-off energy of the plane wave basis set was 60 Ryd. The core electron wavefunctions were represented by the Slater function parameterized by Clementi and Roetti [12]. A self-consistent positron wavefunction was calculated based on the two-component density functional theory in order to minimize the energy functional [8]. The Borónski–Nieminen enhancement factor was adopted. The DBAR spectra were obtained by convoluting one-dimensional angular correlation of the annihilation radiation spectra obtained from the momentum density with the Gaussian resolution function having a half width of $3.92\times10^{-3}$ $m_0c$.

## 4. Results and discussion

Figure 1 shows S-E curves obtained from the HT-GaCrN samples. It is seen that S parameters in both undoped and Si-doped samples are nearly the same as that of the MOCVD GaN template. This suggests that the concentrations of vacancy defects are under the detection limit. In these samples, CrN precipitations are expected to be formed because of high temperature growth. However, the S-E curves exhibit no clear features arising from CrN precipitations.

Figure 2 shows S-E curves obtained from the LT-GaCrN samples. In the case of the undoped GaCrN, S parameter increases significantly. Although the increase in S parameter is suppressed by Si doping, it is still higher than that for the GaN template. This implies that the size and/or number of vacancy defects are reduced by Si doping, but positrons are still trapped by vacancy defects. It seems conceivable that Si atoms, which are occupying Ga sites, will reduce the size and/or number of defects.

From the annihilation lifetime measurement at E=8 keV (average positron implantation depth is 180 nm), the second lifetime component ($\tau_2$=358 ps and $I_2$=21 %) was obtained for the undoped LT-GaCrN. Whereas, the positron lifetime for the Si-doped LT-GaCrN did not show clear increase from that of MOCVD GaN template. Figures 3 and 4 shows the DBAR spectra obtained for the undoped and Si-doped LT-GaCrN samples at E=8 keV. To see the detailed spectrum shape, the original spectra were divided by that of the MOCVD GaN template. The DBAR spectrum for the undoped GaCrN represents a typical feature for vacancy defects. That is, an enhancement in the low momentum region ($p<5\times10^{-3}$ $m_0c$) and a suppression in the high momentum region ($p>10\times10^{-3}$ $m_0c$). Although similar feature is also observed for the Si-doped GaCrN, an additional bump appears at around $p=10\times10^{-3}$ $m_0c$. Thus, different types of vacancy defects are responsible for positron trapping in the undoped and Si-doped GaCrN samples.

Table 1 lists the positron lifetimes calculated for a perfect GaN lattice and some vacancy defects in

GaN. Positron lifetime for a nitrogen vacancy ($V_N$) is 8 ps greater than that for the bulk. Gallium vacancy ($V_{Ga}$) and divacancy ($V_NV_{Ga}$) give rise to sufficiently longer lifetimes than the bulk. With increasing the size of vacancy cluster, positron lifetime is prolonged more. The experimental lifetime for the undoped LT-GaCrN ($\tau_2$=358 ps) is comparable to the calculated lifetimes for $V_8$-$V_{12}$ clusters. As shown in Fig. 3, the experimental DBAR spectrum is also in good agreement with the calculated spectra for $V_8$ and $V_{12}$ clusters. Thus, in the undoped LT-GaCrN, vacancy defects are generated and agglomerated during the growth and subsequent heating at 700°C for the cap layer growth.

In the case of the Si-doped LT-GaCrN, the observed lifetime is very close to that for the GaN template. This means that at least vacancy clusters are ruled out as the candidates for positron trapping. To identify vacancy defects, the calculated DBAR spectra for a series of small vacancy defects ($V_N$, $V_{Ga}$, $V_NV_{Ga}$, $V_N$-$N_{Ga}$, $V_{Ga}$-$Ga_N$, $V_{Ga}$-$Cr_N$, $V_N$-$Cr_{Ga}$, $V_{Ga}$-$Si_N$, $V_N$-$Si_{Ga}$), that are possible from the geometrical viewpoint, are compared with the experimental spectrum. Consequently, it was found that the experimental spectrum is in better agreement with the calculated spectra for nitrogen vacancy related complexes ($V_N$-$N_{Ga}$, $V_N$-$Si_{Ga}$) as shown in Fig. 4. The calculated spectrum for nitrogen vacancy ($V_N$) was closer to the bulk one. Replacement of one Ga atom surrounding a nitrogen vacancy with N or Si provides more space for localizing positrons. Considering the fact that the sample is doped with Si atoms, $V_N$-$Si_{Ga}$ complexes might be a preferred explanation. Possibly, the occupation of Ga sites by Si atoms reduces the amount of gallium vacancies and residual nitrogen vacancies are combined with Si atoms.

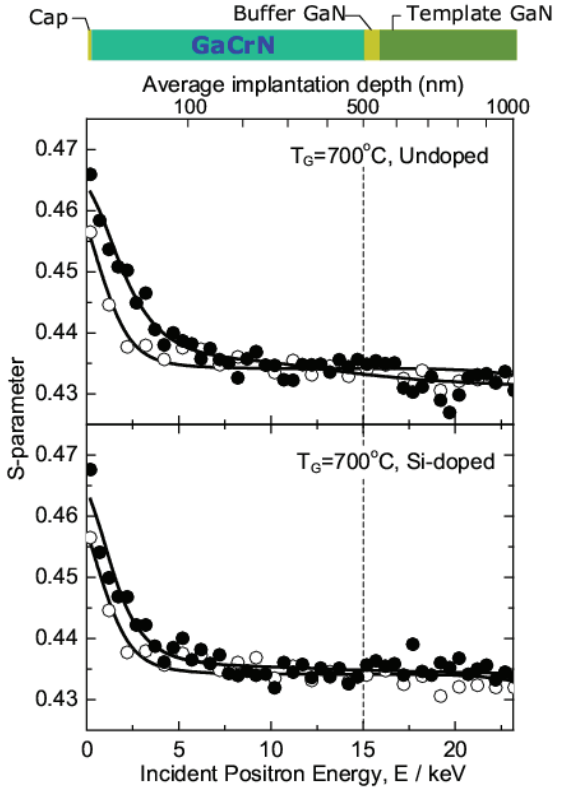


**Figure 1.** S parameter as a function of incident positron energy obtained from the undoped and Si-doped HT-GaCrN samples (filled circles) and the MOCVD GaN template (open circles). The upper horizontal axis denotes the average implantation depth corresponding to the incident positron energy. The top figure schematically shows the structure of samples.

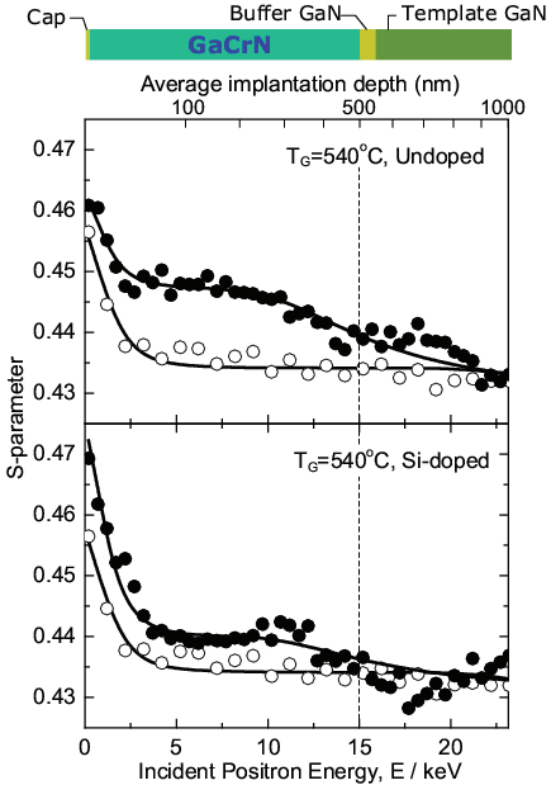


**Figure 2.** S parameter as a function of incident positron energy obtained from the undoped and Si-doped LT-GaCrN samples (filled circles) and the MOCVD GaN template (open circles). The upper horizontal axis denotes the average implantation depth corresponding to the incident positron energy. The top figure schematically shows the structure of samples.

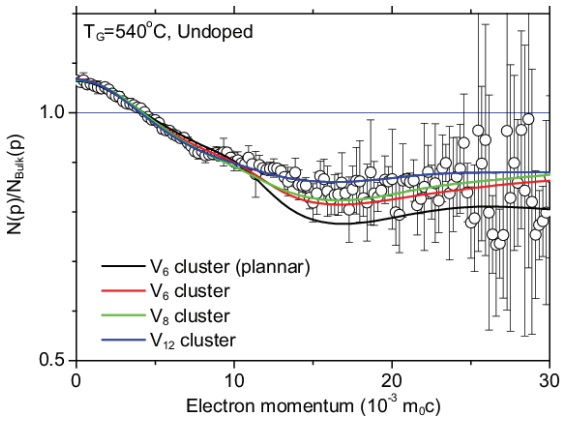


**Figure 3.** DBAR spectrum obtained for the undoped LT-GaCrN at E=8 keV. The original spectrum is divided by the spectrum of MOCVD GaN. Black, red, green and blue solid lines are the calculated DBAR spectra for $V_6$ cluster (planar), $V_6$ cluster, $V_8$ cluster and $V_{12}$ cluster, respectively.

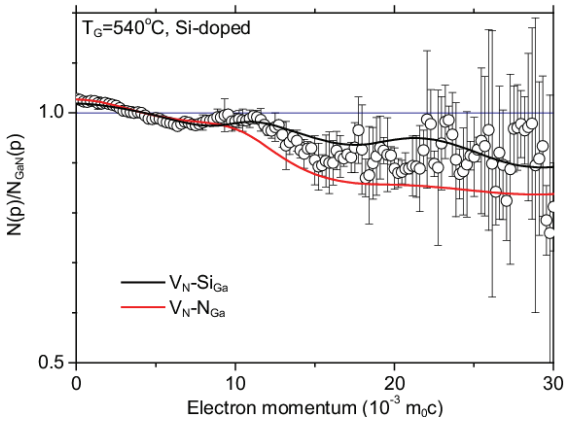


**Figure 4.** DBAR spectrum obtained for the Si-doped LT-GaCrN at E=8 keV. The original spectrum is divided by the spectrum of MOCVD GaN. Black and red solid lines are the calculated DBAR spectra for $V_N$-$Si_{Ga}$ and $V_N$-$N_{Ga}$ complexes, respectively.

Table 1 Positron lifetimes for the perfect GaN lattice and some vacancy defects calculated by the atomic superposition method.

| Bulk | $V_N$ | $V_{Ga}$ | $V_NV_{Ga}$ | $V_6$ | $V_6$ planar | $V_8$ | $V_{12}$ |
|---|---|---|---|---|---|---|---|
| 155 ps | 163 ps | 204 ps | 229 ps | 308 ps | 311 ps | 347 ps | 383 ps |

## 5. Conclusion

In this study, vacancy defects in GaCrN grown by low temperature MBE method have been studied by positron annihilation spectroscopy. It was found that no intentional doping results in the formation of large vacancy clusters during growth. Formation of vacancy clusters could be avoided by intentional Si doping, while complexes related to nitrogen vacancies still survive. The further study is needed to elucidate the effect of vacancy defects on the magnetic properties of GaCrN.

## References

[1] Hashimoto M, Zhou Y K, Kanamura M and Asahi H 2002 *Solid State Commun.* **122** 37-39.
[2] Hashimoto M, Zhou Y K, Kanamura M, Katayama-Yoshida M and Asahi H 2003 *J. Cryst. Growth* **251** 327-330.
[3] Sato K and Katayama-Yoshida H 2001 *Jpn. J. Appl. Phys.* **40** L485-L487.
[4] Kang J and Chang K J 2007 *J. Appl. Phys.* **102** 083910.
[5] Neugebauer J and de Walle C G V 1996 *Appl. Phys. Lett.* **69** 503-505.
[6] Yang X L, Zhu W X, Wang C D, Fang H, Yu T J, Yang Z J, Zhang G Y, Qin X B, Yu R S and Wang B Y 2009 *Appl. Phys. Lett.* **94** 151907.
[7] Puska M J and Nieminen R M 1994 *Rev. Mod. Phys.* **66** 841–897.
[8] Borónski E and Nieminen R M 1986 *Phys. Rev.* B **34** 3820–3831.
[9] Blöhl P E 1994 *Phys. Rev.* B**50** 17953-17979.
[10] Gonze X, Beuken J -M, Caracas R, Detraux F, Fuchs M, Rignanese G -M, Sindic L, Verstraete M, Zerah G, Jollet F, Torrent M, Roy A, Mikami M, Ghosez Ph, Raty J -Y, and Allan D C 2002 *Comput. Mater. Sci.* **25** 478–492.
[11] Holzwarth N A W, Tackett A R and Matthews G E 2001 *Comput. Phys. Commun.* **135** 329–347.
[12] Clementi E and Roetti C 1974 *At. Data Nucl. Data Tables* **14** 177-478.